



SEAWATER INTRUSION INTO GROUNDWATER COSTAL AQUIFERS AT AL- QUNFUDAH PROVINCE, WESTERN SAUDI ARABIA

Khaled O Al-GADI

Master Degree in Science in Geographic Information System, King Abdulaziz
University, Jeddah Saudi Arabia

E-mail: kalgadi86@gmail.com

Dr. Mahmoud Al-Doaan

Department of Geography Faculty of Arts & Humanities King Abdulaziz University,
Jeddah Saudi Arabia

E-mail: mdoaan@kau.edu.sa

ABSTRACT

Seawater intrusion into groundwater aquifer is an issue that adversely affects freshwater resources and infrastructure. This phenomenon particularly exacerbated in the coastal cities through the exploitation of groundwater for agricultural activity and development. The determination of hazardous zones and the extension of seawater intrusion is critical to identify the affected areas and to contribute to developing appropriate solutions. This study aims to assess the extent of Seawater intrusion on the coastal aquifers in Al Qunfidhah Province. The objective is to identify areas of vulnerability using geographic information systems (GIS) to generate maps of seawater intrusion into groundwater using a groundwater quality index specific for seawater intrusion (GQISWI) to build a variogram model. GIS can help to make the results of complex models more visible through visual representation, providing a viable tool for decision-makers. The effect range map shows three categories: low, moderate, and high, depending on groundwater quality index specific for seawater intrusion (GQISWI). These maps can be used as preliminary maps to plan detailed studies to monitor interference as well as sustainable land use planning and groundwater management in Al Qunfidhah Province.

Keywords: seawater intrusion, groundwater aquifer, coastal aquifers, Al Qunfidhah Province.

تداخل مياه البحر الأحمر لتكوينات المياه الجوفية الساحلية بمحافظة القنفذة غرب المملكة العربية السعودية

الملخص

تداخل مياه البحر الى طبقات المياه الجوفية ظاهرة تؤثر بشكل سلبي على موارد المياه العذبة والبنية التحتية. تتفاقم هذه الظاهرة في المدن الساحلية من خلال استغلال المياه الجوفية في النشاط الزراعي والتنمية. تحديد المناطق المتضررة من توسع ظاهرة تداخل مياه البحر امر بالغ الاهمية للمساهمة في تطوير الحلول المناسبة. تهدف هذه الدراسة الى تقييم امتداد تداخل مياه البحر على المياه الجوفية الساحلية في محافظة القنفذة وتحديد مناطق الضعف باستخدام نظم المعلومات الجغرافية (GIS) لإنشاء خرائط لتداخل مياه البحر على المياه الجوفية باستخدام مؤشر جودة المياه الجوفية المحدد لتسرب مياه البحر (GQISWI). يمكن ان تساعد نظم المعلومات الجغرافية في جعل النماذج المعقدة أكثر وضوحاً من خلال التمثيل المرئي، مما يوفر أداة قابلة للتطبيق لصناع القرار. تظهر خريطة نطاق التأثير ثلاث فئات : منخفضة ومتوسطة وعالية، اعتماداً على مؤشر جودة المياه الجوفية المحدد لتسرب مياه البحر (GQISWI). يمكن استخدام هذه الخرائط للتخطيط لدراسات تفصيلية لرصد التداخل وكذلك التخطيط المستدام لإستخدام الأراضي وإدارة المياه الجوفية في منطقة القنفذة.

INTRODUCTION

Overview

The constant supply of freshwater is critical for ensuring a good life. It also contributes to economic growth and environmental sustainability in urban areas. Approximately a third of our source for drinking and living purposes water supply is groundwater. (Dávila Pórcel, De León Gómez and Schüth, 2011). The hydrochemical differentiation of the salinization processes is very complex as there is considerable hydrochemical variability due to the superposition of different processes: marine intrusion, recycling of wastewaters, continental saltwater contribution and pollution phenomena by agricultural activities (Zghibi et al., 2014).

The phenomenon of groundwater salinization due to Seawater intrusion in the coastal cities is a threat to groundwater. Seawater intrusion occurs mainly due to over pumping/ extraction of freshwater and Sea-level Rise, which causes lateral and vertical movements of seawater into the coastal aquifers. (Sridharan and Senthil Nathan, 2017). Seawater and freshwater have different hydrochemistry, with seawater characterized by nearly regular chemistry where chloride (Cl^-) and sodium (Na^+) represent 84% of the total ionic composition. On the other hand, the freshwater composition varies, usually dominance by calcium (Ca^{2+}) and bicarbonate (HCO_3^-) (Tomaszkiewicz, Abou Najm and El-Fadel, 2014).

Study area

Al Qunfidhah City lies on the Red Sea coast at downstream of Wadi Qanuna Basin. Wadi Qanuna is one of the largest wadis in the South-West of Saudi Arabia, with a total length of about 108 kilometers. (Facts and figures 2017 Saudi Geological Survey). This wadi begins from the high mountains of the Hijaz West heading in the flow downward towards the Red Sea passing through Al-Qunfidhah city. The average slope of Wadi Qanuna is about 10.7 m/km (1:250,000 Topographic map, Ministry of petroleum and mineral resources 1980).

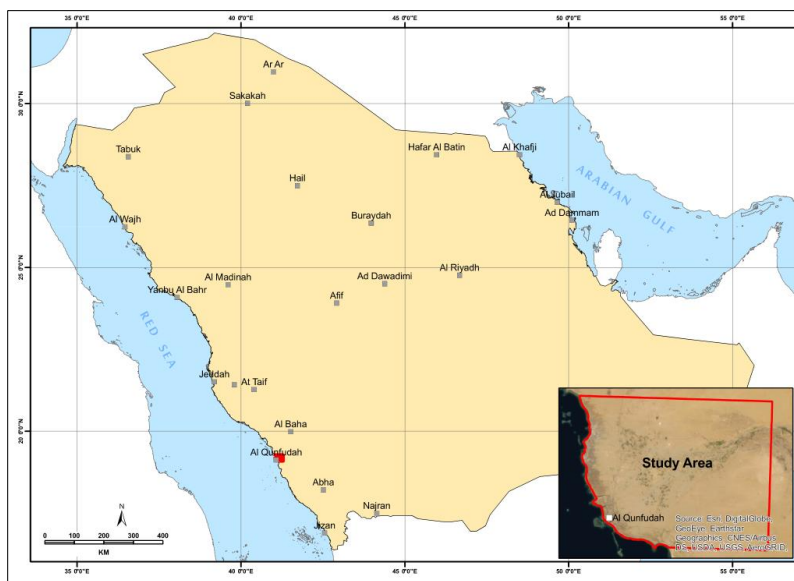


Figure 1: Location map

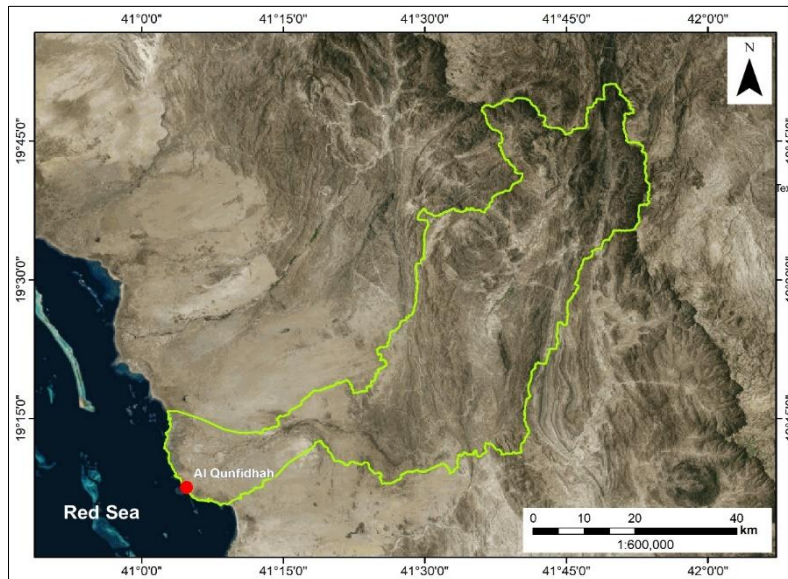


Figure 2: Qunouna Basin

Methodology

- Collecting data for the study area; topography, wells location, and hydrochemical analysis.
- Applying the statistical analysis for groundwater physical parameters; Electrical conductivity (EC), Total dissolved solids (TDS), pH, and the depth to water, in addition to and the chemical composition of groundwater (cations and anions).
- Applying QGIswi, which extracts from hydrochemical technics and theory to determines contribution of Seawater into groundwater.
- Applying geographic information system as the following:
 - Spatial analysis for EC using spatial autocorrelation (MoransI) to find out if we have a cluster and define high cluster area.
 - Spatial interpolation methods were used to create the intrusion map.

Hydrogeological data

According to the information collected from the project of Groundwater Rise hazards in Makkah Region (unpublished report 2017 by Saudi Geological Survey). The study area is formed mostly from alluvial deposits. The aquifer is unconfined and shallow that directly recharged by rainfall and occasional floods. Most of the rainfall appears as runoff and flows towards the Red Sea through Al Qunfidhah where the quaternary deposits, areal extension, and thickness are comparatively small. Floods from Qunouna Basin constitute a significant source of groundwater recharge. High infiltration rates are enough to fill the alluvial deposits in a short time, and consequently, at places of high permeability, there appear surface water depressions that are directly connected to shallow unconfined aquifers.

As the Red Sea coastal area is approached, the groundwater quality deteriorates and becomes very saline due to seawater intrusion. On-site measurements of temperature, electric conductivity (EC), alkalinity, pH, and redox potential (Eh) were taken for the groundwater sampling point in the study area figure (3). Additionally, groundwater samples were analyzed at the Saudi Geological Survey Laboratory using inductively coupled plasma mass spectrometry (ICP-MS).

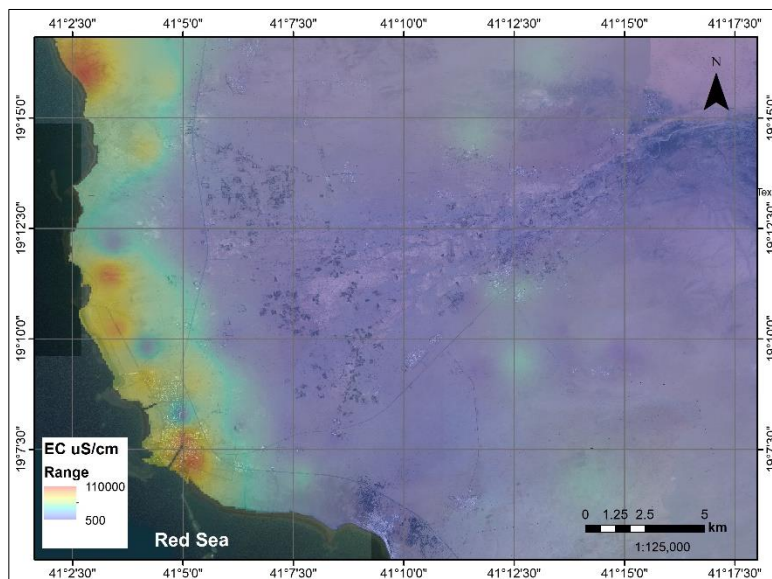


Figure 3: EC distribution in the ground water sample

Hydrochemical Analysis



The groundwater quality takes its final chemical compositional structure depending on the types of rocks that it crosses through. The knowledge about the chemical composition of different rock types in the area reflects the physical features of the hydrochemistry of the groundwater samples collected in the field. The rocks have a unique and direct effect on the alteration of groundwater chemistry. It is possible to infer from the hydrochemical analysis to a certain extent what the possible rock types are or vice versa. They also help to detect and identify any other sources affecting groundwater such as Seawater intrusion.

Seawater and freshwater are characterized by various aquatic chemistry, the first being characterized by almost identical chemistry where chloride (Cl⁻) and sodium (Na⁺) make up to 84% of the total ionic composition. Moreover, the composition of freshwater varies widely, with calcium (Ca²⁺) and bicarbonate (HCO₃⁻) dominating. Mixing this water is usually depicted by increasing the concentration of Cl⁻ within the aquifer, which can be easily traced due to the conservative nature of the anion. In fact, the fraction of seawater (f_{sea}) in a water sample can be approximated by the concentrations of Cl⁻ (mCl) (in meq/l) as shown in the equation (1). (Appelo and Postma, 2005) Table (1) shows Classification of groundwater Adapted from Konikow and Reilly, 1999; Rhoades et al., 1992.

$$(1) \Rightarrow F_{sea} = \frac{m_{Cl(sample)} - m_{Cl(freshwater)}}{m_{Cl(seawater)} - m_{Cl(freshwater)}}$$

Table 1: Classification of groundwater

Class	Cl (meq/l)	TDS (ppm)	EC
Fresh groundwater	<2.8	0-500	<700
Slightly saline	2.8-7.1	500-1500	700-2000



groundwater			
Moderately saline	7.1-14.1	1500-7000	2000-10000
Highly saline groundwater	14.1-28.2	7000-15000	10000-25000
Very Highly saline groundwater	28.2-282.2	15000-35000	25000-45000
Seawater	>282.2	>35000	45000

Adapted from [Konikow and Reilly, 1999; Rhoades et al., 1992](#).

Piper diagram groundwater quality indices

The diamond field in the Piper diagram is divided into six different zones: I, II, III, IV, V, and VI, which can demonstrate CaHCO₃, NaCl, mixed CaNaHCO₃, mixed CaMgCl, CaCl, and NaHCO₃, mixed waters respectively see figure(4) (Subramani et al. 2005; Sarat Prasanth et al. 2012). Freshwater is generally illustrated in the I zone, while saline water, including seawater, is in the II zone. The simple mixing of freshwater and seawater is indicated by a horizontal line across the centre of the diagram that is given a numerically by GQI_{piper} (mix) as shown in equation (2):

$$(2) \Rightarrow \text{GQI}_{\text{piper}}(\text{mix}) = \left[\frac{(\text{Ca}^{2+} + \text{Mg}^{2+})}{\text{Total cations}} + \frac{(\text{HCO}_3^-)}{\text{Total anions}} \right] \times 50 \text{ (in meq/l)}$$

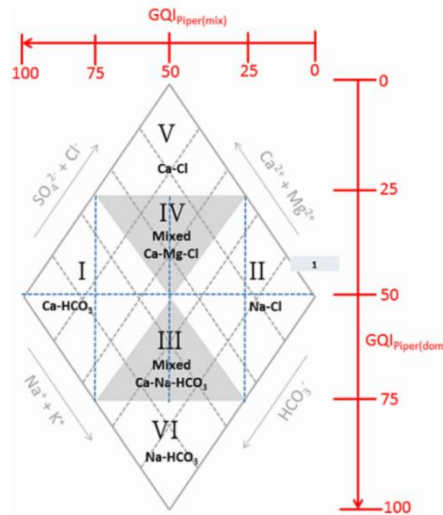


Figure 4: The GQI_{piper} (mix) and GQI_{piper} (dom)

The output of GQI_{piper}mix ranges from 0, illustrate extremely saline water (zone II), to 100, illustrate extremely freshwater (zone I). Further definition of the other domains in Figure (4) can be accomplished when GQI_{piper} (mix) is used as the same time with another index, GQI_{piper}dom (Equation (3)), that equally ranges from 0, demonstrating CaCl water (zone V), to 100, demonstrating NaHCO₃ type waters (zone VI).

$$(3) \Rightarrow \text{GQI}_{\text{piperdom}} = \left[\frac{(\text{Na} + +\text{K}+)}{\text{Total cations}} + \frac{(\text{Hco}3-)}{\text{Total anions}} \right] \times 50 \text{ (in meq/l)}$$

The ranges of GQI_{piper} (mix) and GQI_{piper} (dom) and the corresponding hydrogeochemical zones are presented in table (2). to define hydrogeochemical water zones based on measured water quality data. (Tomaszkiewicz, Abou Najm and El-Fadel, 2014).

Table2: Ranges of GQI_{piper}(mix) and GQI_{piper}(dom)

Zone	GQI _{piper} mix	GQI _{piper} dom
I	50-100	25-75
II	0-50	25-75



III	25-75	50-75
IV	25-75	25-50
V	25-75	0-25
VI	25-75	75-100

Seawater fraction as a groundwater quality index

The fraction of seawater (FSEA) consider as another common tool for determining seawater intrusion with values ranging from 0 to 100 by definition, which gives itself easily towards the GQIfsea index, where freshwater has less FSEA (equation (4)). Locally measured Cl concentrations are permanently used to estimate fsea to reduce background Cl impact. When the Cl is not available, it can be assumed that it equals 0-566 meq/ l for freshwater or seawater, respectively. (Appelo and Postma, 2005).

$$(4) \Rightarrow F_{sea} = 1 - F_{sea} \times 100$$

Like the Piper diagram, FSEA has weaknesses and might not be an appropriate indicator independently. It fails to identify most of the hydro-chemical reactions associated with seawater leakage, such as cation exchange, which can affect the numerical composition of aquifers subject to overflow of seawater more than concentrations - on which FSEA depends. Also, cl- content can increase by nearly 1% three times the salinity of groundwater, especially if the background concentration is low, indicating a high sensibility to the parameter. Moreover, alkaline water can be less salty, even with a higher FSEA existence. (Bakari et al., 2011).

Groundwater quality index specific for seawater intrusion (GQISWI)

In this study, we use the combination of FSEA and GQIPiper results (mix) which could be a more representative indicator of seawater mixing. The GQISWI is index (equation (5)) and is equally derived from the values of GQIPiper (mix) (equation (2)) and GQIfsea



(equation (4)) to guarantee that recompense the strengths in one index the weaknesses in another (Fig. 4)). (Tomaszkiewicz, Abou Najm and El-Fadel, 2014).

$$(5) \Rightarrow GQI_{swi} = GQI_{pipermix} + GQI_{fsea}/2$$

Statistical Analysis

Descriptive statistics & Exploratory Data Analysis

In descriptive statistics, Data can be described with frequency distributions and other measures such as range, minimum, maximum, mean value, variance & standard deviation, skewness, and kurtosis see table (3). EDA (Exploratory Data Analysis) Statistics that tries to maximize the insight into complex data sets by uncovering the underlying trends and structures and detecting outliers such as boxplot (which can represent five quantities for a set of data: the **median**; the first **quartile** and the third quartile; the maximum and minimum **values**) (Dodge, 2008).

Table 3: Statistical summary

	N	Range	Minimum	Maximum	Mean	Std. Deviation	Variance	Skewness	Kurtosis
EC	95	112384.00	916.00	113300.00	19380.20	28851.92	832433312.35	2.11	3.48
TDS	95	88069.23	591.30	88660.53	14509.67	22304.50	497490704.05	2.25	4.14
Ph	95	742.23	6.77	749.00	15.27	76.08	5788.27	9.75	95.00
Depth_to_water	95	64.97	1.04	66.00	10.88	8.30	68.95	3.21	19.56
Ca	95	2174.27	30.68	2204.95	410.38	423.20	179098.73	1.91	3.74
Mg	95	2881.51	11.89	2893.40	378.74	568.91	323663.37	2.52	6.67
Na	95	29868.93	49.00	29917.93	4398.32	7550.06	57003417.39	2.34	4.56
K	95	1803.60	0.01	1803.61	226.65	384.62	147930.33	2.31	4.86
Cl	95	53406.70	72.30	53479.00	7503.97	12898.30	166366018.08	2.34	4.55
HCO3	95	526.00	83.00	609.00	258.71	115.60	13362.87	1.03	0.71
NO3	95	105.99	0.01	106.00	18.94	23.31	543.46	1.84	3.05
SO4	95	6447.00	133.00	6580.00	1311.51	1217.53	1482380.25	1.77	3.68



The frequency distribution of my data doesn't entirely overlap with their normal curves. The histograms and their curves do not take the shape of the bell, so we tested by applying tests of Normality by Kolmogorov-Smirnov and Shapiro-Wilk (Mohd Razali and Wah Yap, 2011).

Table 4: Tests of Normality

	Kolmogorov-Smirnov ^a			Shapiro-Wilk		
	Statisti c	df	Sig.	Statisti c	df	Sig.
EC	.287	95	.000	.642	95	.000
Ph	.526	95	.000	.080	95	.000
TDS	.266	95	.000	.626	95	.000
Water level	.119	95	.002	.762	95	.000
Ca	.205	95	.000	.762	95	.000
Mg	.273	95	.000	.641	95	.000
Na	.282	95	.000	.596	95	.000
K	.278	95	.000	.629	95	.000
Cl	.284	95	.000	.600	95	.000
HCO3	.151	95	.000	.920	95	.000
NO3	.228	95	.000	.735	95	.000
SO4	.195	95	.000	.812	95	.000

a. Lilliefors Significance Correction

Kolmogorov-Smirnov testing if a variable follows a normal distribution in a population. It reflects in one number how different my data is from a zero hypothesis. Therefore, it indicates the extent to which observed data deviate from normal distribution. So, a **large deviation has a low p-value, and low deviation has high p-value.**

If $p < 0.05$, we don't believe that our variable follows a normal distribution in our population. As shown in the above table, all significant value less than 0.05 which mean they don't follow normal distribution shows in table (4).

Spatial Analysis

Spatial characteristics of the data set such as central tendency, spread and direction. Analysis that shows the mean center of the sample, and the standard deviation ellipse (showing the directional trend). The mean center is the average x and y coordinate of all the features in the study area. It's useful for tracking changes in the distribution or for comparing the distributions of different types of features. Central Feature: Identifies the most centrally located feature in a point, line, or polygon feature class. The Standard Distance tool (displayed graphically as a circle) is calculated using the distance of each well from the calculated center.

Directional Distribution: Creates standard deviational ellipses or ellipsoids to summarize the spatial characteristics of geographic features: central tendency, dispersion, and directional trends.

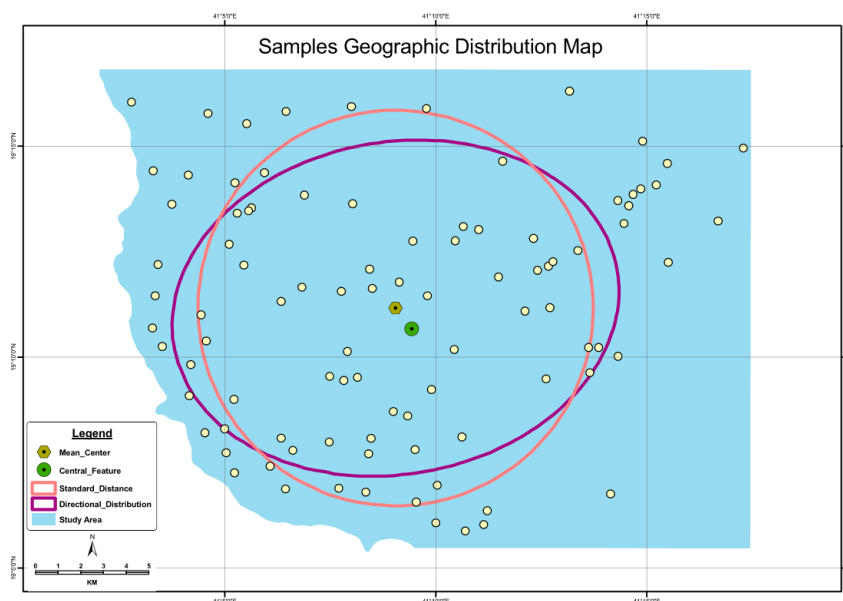


Figure 5: Sample Geographic Distribution Map

Patterns Analysing



Moran’s Index and z-score show in the figure show that we have a significant cluster. So, we have to identify at what scale or distance the autocorrelation maximizes. (distance at which cluster maximizing) However, to do so we need to know at which distance at least we have one neighbor the function to do [calculate distance band from neighbor count]

As we can see, the minimum distance to find one neighbor is 169 meters but, what is really we need is the average distance at least for one neighbor, which equals to 1240 meters will be used in the Incremental spatial autocorrelation function. Incremental spatial autocorrelation function measures spatial autocorrelation for a series of distance and draws a graph line showing distances and corresponding values of z-scores.

Global Moran's I Summary by Distance

Distance	Moran's Index	Expected Index	Variance	z-score	p-value
1240.00*	0.437311	-0.016129	0.017084	3.469125	0.000522
1840.00*	0.475165	-0.012048	0.007838	5.503195	0.000000
2440.00*	0.586615	-0.011494	0.004461	8.954535	0.000000
3040.00*	0.550982	-0.011111	0.003026	10.218378	0.000000
3640.00*	0.416052	-0.010638	0.002154	9.192928	0.000000
4240.00*	0.384215	-0.010526	0.001479	10.264039	0.000000
4840.00*	0.349265	-0.010526	0.001192	10.421482	0.000000
5440.00	0.302086	-0.010417	0.000910	10.357174	0.000000
6040.00	0.262697	-0.010417	0.000725	10.145046	0.000000
6640.00	0.228606	-0.010417	0.000589	9.845210	0.000000

First Peak (Distance, Value): 3040.00, 10.218378

Max Peak (Distance, Value): 4840.00, 10.421482

Distance measured in Meters

* At least one distance increment resulted in features with no neighbors which may invalidate the significance of the corresponding results.

Figure 6: Spatial autocorrelation

Statistically significant peak z-scores Indicates the distances to spatial processes promoting clustering are most pronounced. These peak distances are often appropriate values to use for tools with a Distance Band or Distance Radius parameter. Max Peak 4840m that where you find maximum clustering, and now we can do cluster and outlier analysis, and this will generate a map of the hot spot.

Spatial interpolation



There are several types of interpolation methods used in creating surfaces Thiessen polygons, Inverse Distance Weighted (IDW), Natural Neighbour Inverse Distance Weighted (NNIDW), Spline, Kriging, and Trend. (Tan, Qulin & Xu, Xiao.,2014).

Deterministic and geostatistical techniques are used to understand the spatial variation of groundwater. (KUMARI et al., 2018) We did perform one of deterministic, which Inverse Distance Weighted (IDW), selected as the simplest procedure and one of the geostatistical, which is ordinary kriging is the most commonly used.

Inverse Distance Weighted (IDW)

IDW method supposes that the averages of correlation between neighbors are symmetrical to the distance between them. Applying IDW for our variables of interest QGIswi, the out but sell size as the area of study with the default input point will be used to interpolate the value for each cell in the output raster as shown in figure (20).

Kriging interpolation

Ordinary Kriging use semivariogram to measure the average degree of dissimilarity between no sampled values and nearby data value, and depict autocorrelation at a various distance.

$$Z(s) = \mu + \varepsilon(s)$$

where μ is an unknown constant. One of the main issues concerning ordinary kriging is whether the assumption of a constant mean is reasonable. Sometimes there are good scientific reasons to reject this assumption. However, as a simple prediction method, it has remarkable flexibility.

Semivariogram:

In order to find the best model, we test several models to fit our data. Finally, we decided to choose Bessel K as shown in figure (21).

Choice of Neighborhood



Many different sizes and the optimal number of samples were tested using punctual estimation comparing the weighted attached to the mean near to zero and the slope of the regression Z / Z^* near to one figure (24) shows the result.

Negative weight

The negative weight is typically very small negative values and usually does not create any problems. However, the small negative weight is applied to relatively high value. This means a high negative contribution to the overall kriged value, which can result in a negative estimate (see The Art and Science of Resource Estimation By Jacqui Coombes 2008).

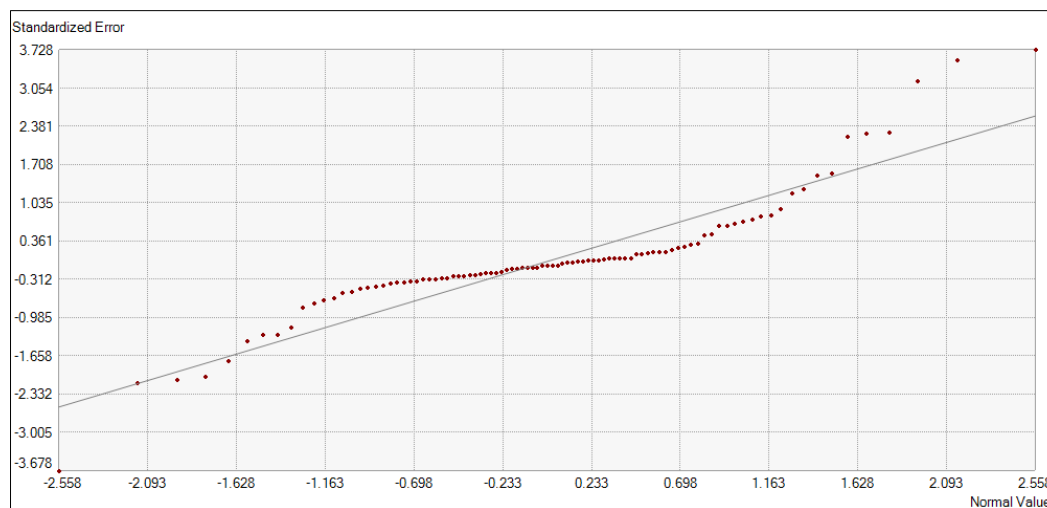


Figure 7: Normal q-q plot

The mean of standardized error close to zero and it is variance close to one.

Regression function $0.571368811596074 * x + 22.4397084110537$

Prediction Errors

Samples 95 of 95



Mean 0.9717759522148266

Root-Mean-Square 21.112321324306798

Mean Standardized 0.03365657839978571

Root-Mean-Square Standardized 1.0566174745528134

Average Standard Error 19.338247730312652

Result and discussion

From the statistical analysis, we found the Correlation between EC and TDS is significant at the 0.01 level (2-tailed). The scatterplot shows the Positive relationship all point assembling around the line figure (8) so we don't need to perform cluster analysis on both EC and TDS.

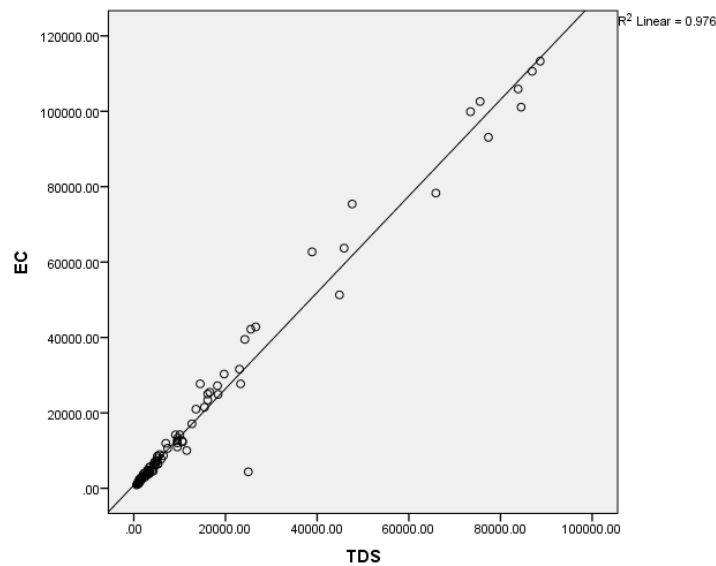


Figure 8: Scatterplot for EC and TDS

We chose to perform the cluster analysis on EC and the result is shown in figure (9), demonstrating the area with high electric connectivity (EC). The values of EC which classified as high cluster ranges between 39500 to 113300 and these values according to

the table Adapted from Konikow and Reilly, 1999; Rhoades et al., 1992 table (2) are classified as very high saline groundwater and seawater.

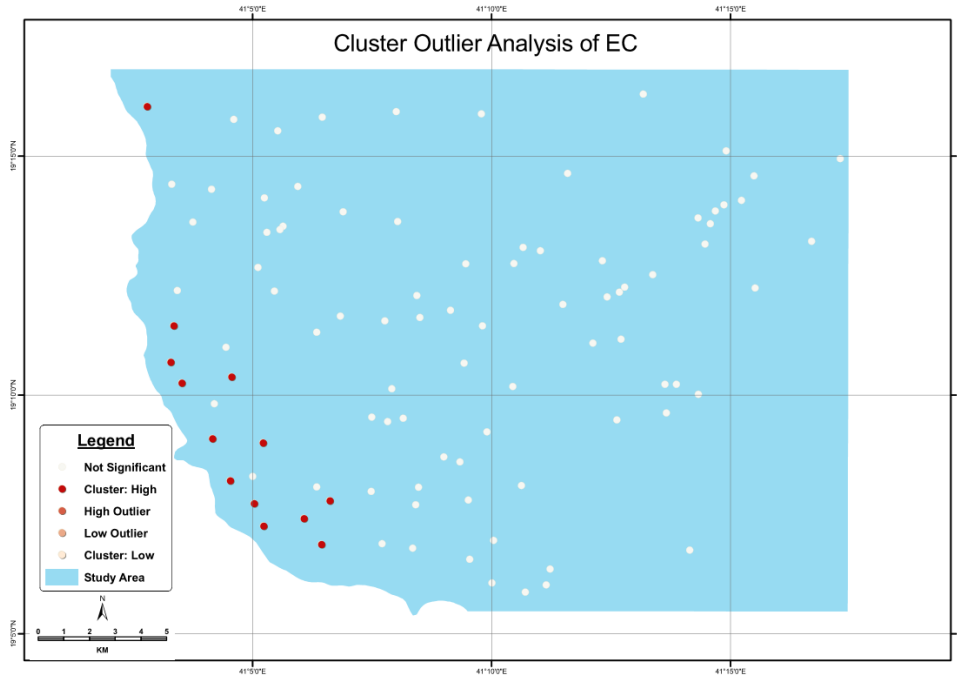


Figure 9: Cluster Analysis

Figure (9) show map of Anselin local moran’s I, and we can recognize the high cluster sample redpoint it means high value of EC around each other. On the other hand, one blue point indicates a low outlier point, which mean the value of EC less than their neighbor.

The following table (5) demonstrated a newly proposed groundwater quality index specific for seawater intrusion (GQISWI) derived by combining the seawater fraction index (GQIfsea) and the freshwater seawater mixing index (GQIPiper (mix)) of the Piper diagram, showing a more representative performance over each factor alone. (Tomaszkiewicz, Abou Najm and El-Fadel, 2014).

**Table 5: GQISWI ranges**

Water type	GQISWI based on worldwide literature			Typical GQISWI	
	Min	Max	Mean	Min	Max
Freshwater	73.5	90.1	82.7	75	100
Mixed groundwater	47.8	79.9	63.4	50	75
Saline groundwater	4.8	58.8	27.5	10	50
Seawater	3.1	9.2	5.8	0	10

Tomaszkiewicz et al. / Environmental Modelling & Software 57 (2014) 13e26

Both interpolation of Deterministic and geostatistical techniques show approximately same result for the coastal area and the shades of red represent variation of Seawater intrusion in figure (10). Inverse Distance Weighted (IDW), and figure (11) Ordinary Kriging.

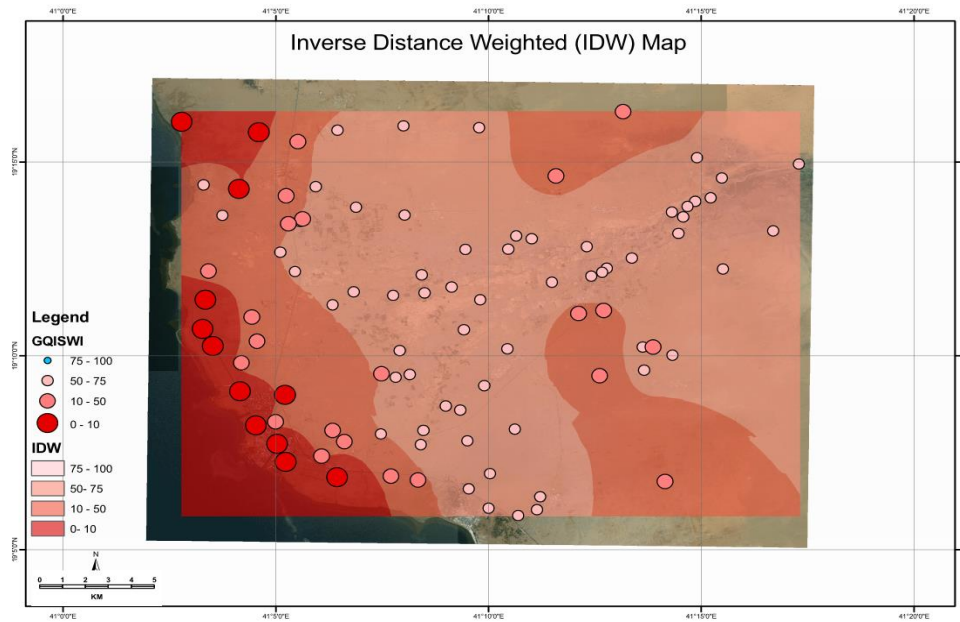
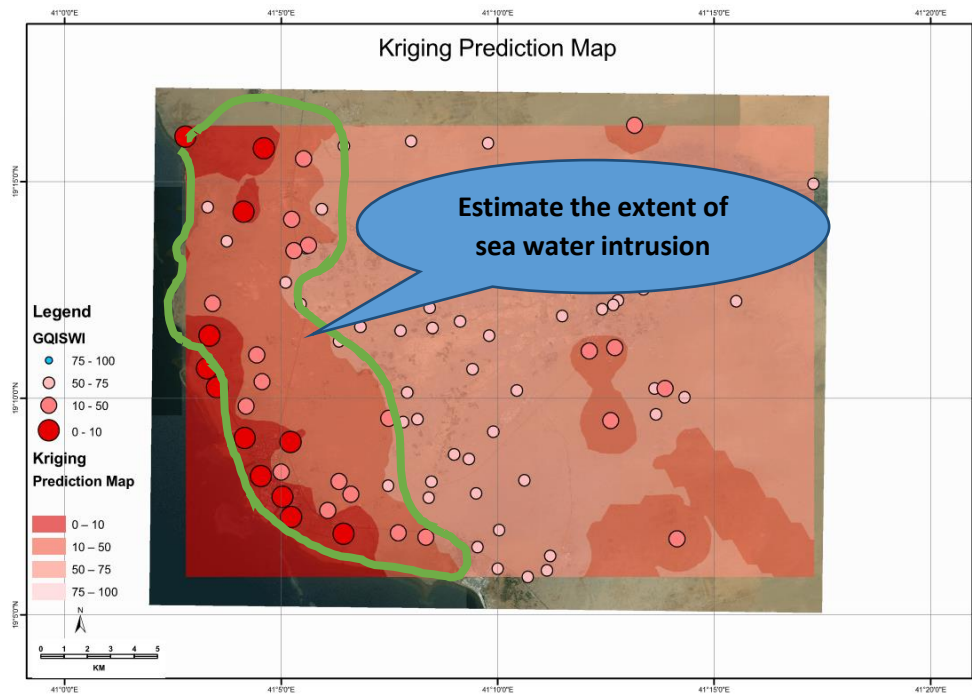


Figure 9: I DW Map



Kriging Map

Conclusion



The objective is to identify areas of vulnerability using geographic information systems (GIS) to generate maps of seawater intrusion into groundwater using a GQISWI to build a variogram model. GIS can help to make the results of complex models more visible through visual representation, providing a viable tool for decision-makers. The goal of the GIS-based index is to rapidly aggregate chemical data into a quantifiable value that can be spatially and temporally mapped. However, the effect range map shows three categories: mixed, saline groundwater, and seawater, depending on GQISWI.

The resulting maps provide by geographic information system a helpful visual tool for researchers and decision-makers towards defining corrective or adaptive measures. The early seawater intrusion is evident in the western quadrant of the study area is alarming, as the groundwater is a source for domestic use.

- There is no fresh water in the study area and the salinity levels vary from seawater to saline groundwater and mixed salinity.
- It turns out that the water in the study area is not suitable for humans, and maybe suitable for some types of animals.
- In the eastern part of the study area, the mixed groundwater zone is suitable for growing certain types of crops.

Reference

Dávila Pórcel, R., De León Gómez, H. and Schüth, C. (2011). Urban impacts analysis on hydrochemical and hydrogeological evolution of groundwater in shallow aquifer Linares, Mexico. *Environmental Earth Sciences*, 66(7), pp.1871-1880.

Sridharan, M. and Senthil Nathan, D. (2017). Hydrochemical Facies and Ionic Exchange in Coastal Aquifers of Puducherry Region, India: Implications for Seawater Intrusion. *Earth Systems and Environment*, 1(1).

Zghibi, A., Merzougui, A., Zouhri, L. and Tarhouni, J. (2014). Understanding groundwater chemistry using multivariate statistics techniques to the study of contamination in the Korba unconfined aquifer system of Cap-Bon (North-east of Tunisia). *Journal of African Earth Sciences*, 89, pp.1-15.



Tomaszkiewicz, M., Abou Najm, M. and El-Fadel, M. (2014). Development of a groundwater quality index for seawater intrusion in coastal aquifers. *Environmental Modelling & Software*, 57, pp.13-26.

Rick Brassington. (n.d.). *Field Hydrogeology* (2017th ed.). John Wiley & Sons Ltd.

Bear, J. (2011). *Seawater intrusion in coastal aquifers*. 7th ed. Dordrecht: Springer.

Werner, A., Bakker, M., Post, V., Vandenbohede, A., Lu, C., Ataie-Ashtiani, B., Simmons, C. and Barry, D. (2013). Seawater intrusion processes, investigation and management: Recent advances and future challenges. *Advances in Water Resources*, 51, pp.3-26.

Tiruneh, N. (2004). Simulation and optimization of seawater intrusion in coastal aquifers due to climate change and sea level rise. p.217.

Trabelsi, N., Triki, I., Hentati, I. and Zairi, M. (2016). Aquifer vulnerability and seawater intrusion risk using GALDIT, GQISWI and GIS: case of a coastal aquifer in Tunisia. *Environmental Earth Sciences*, 75(8).

Tomaszkiewicz, M., Abou Najm, M. and El-Fadel, M. (2014). Development of a groundwater quality index for seawater intrusion in coastal aquifers. *Environmental Modelling & Software*, 57, pp.13-26.

Villholth K.G. (2013) *Integrated Groundwater Use and Management in Vulnerable Coastal Zones of Asia-Pacific*. In: Wetzelhuetter C. (eds) *Groundwater in the Coastal Zones of Asia-Pacific*. Coastal Research Library, vol 7. Springer, Dordrecht

Freeze, R. and A.Cherry, J. (1979). *Groundwater*. 1st ed. [e-book] United States of America: Prentice-Hall. Inc., Englewood Cliffs, N.J. 07632, p.624.

Geography, its subject, approaches and objectives. First edition (2000), Damascus: Dar Al-Fikr / p. 528

Dr. Al-Azzawi, (2013). *Spatial statistical analysis in geographic information systems*



[online] Swideg-geography.blogspot.com. Available at: <http://swideg-geography.blogspot.com/2013/08/e-mail-ail-azawy2000yahoo.html> [Accessed 23 Feb. 2019].

Dodge, Y. (2008). *The Concise Encyclopedia of Statistics*. New York: Springer.

Singhal, B. and Gupta, R. (2010). Groundwater Quality. *Applied Hydrogeology of Fractured Rocks*, [online] pp.205-220. Available at: https://link.springer.com/chapter/10.1007/978-90-481-8799-7_11#citeas [Accessed 5 Oct. 2019].

Singhal, B. and Gupta, R. (2010). Groundwater Quality. *Applied Hydrogeology of Fractured Rocks*, pp.205-220.

Appelo, C. and Postma, D. (2005). *Geochemistry, groundwater and pollution*. 2nd ed. Leiden: Balkema.

Bakari, S., Aagaard, P., Vogt, R., Ruden, F., Johansen, I. and Vuai, S. (2011). Delineation of groundwater provenance in a coastal aquifer using statistical and isotopic methods, Southeast Tanzania. *Environmental Earth Sciences*, 66(3), pp.889-902.

Tan, Qulin & Xu, Xiao. (2014). Comparative Analysis of Spatial Interpolation Methods: an Experimental Study. *Sensors and Transducers*. 165, pp.155-163.

Piazza, A., Conti, F., Viola, F., Eccel, E. and Noto, L. (2015). Comparative Analysis of Spatial Interpolation Methods in the Mediterranean Area: Application to Temperature in Sicily. *Water*, 7(12), pp.1866-1888.

KUMARI, M., SAKAI, K., KIMURA, S., NAKAMURA, S., YUGE, K., GUNARATHNA, M., RANAGALAGE, M. and DUMINDA, D. (2018). INTERPOLATION METHODS FOR GROUNDWATER QUALITY ASSESSMENT IN TANK CASCADE LANDSCAPE: A STUDY OF ULAGALLA CASCADE, SRI LANKA. *Applied Ecology and Environmental Research*, 16(5), pp.5359-5380.

The Art and Science of Resource Estimation by Jacqui Coombes, Coombes Capability 2008.